Journal of the American Heart Association

ORIGINAL RESEARCH

COL5A1 Variants Cause Aortic Dissection by Activating TGF-β-Signaling Pathway

Peng Chen, MD, PhD*; Bo Yu, MD, PhD*; Zongzhe Li, MD, PhD; Yanghui Chen, MD; Yang Sun, MD, PhD; Dao Wen Wang, MD, PhD

BACKGROUND: Aortic dissection (AD) is one of the most life-threatening cardiovascular diseases that exhibit high genetic heterogeneity. However, it is unclear whether variants within the *COL5A1* gene can cause AD. Therefore, we intend to determine whether *COL5A1* is a causative gene of AD.

METHODS AND RESULTS: We performed targeted sequencing in 702 patients with unrelated sporadic AD and 163 matched healthy controls using a predesigned panel with 152 vessel matrix-related genes. As a result, we identified that 11 variants in *COL5A1* caused AD in 11 out of the 702 patients with AD. Furthermore, *Col5a1* knockout (*Col5a1*$^{+/-}$) rats were generated through the CRISPR/Cas9 system. Although there was no spontaneous AD, electron microscopy revealed a fracture of elastic fibers and disarray of collagenous fibers in 6-week-old *Col5a1*$^{+/-}$ rats, but not in WT rats (93.3% versus 0.0%, $P<0.001$). Three-week-old rats were used to induce the AD phenotype with β-aminopropionitrile monofumarate for 4 weeks followed by angiotensin II for 72 hours. The β-aminopropionitrile monofumarate and angiotensin II-treated rat model confirmed that *Col5a1*$^{+/-}$ rats had considerably higher AD incidence than WT rats. Subsequent mechanism analyses demonstrated that the transforming growth factor-β-signaling pathway was significantly activated in *Col5a1*$^{+/-}$ rats.

CONCLUSIONS: Our findings, for the first time, revealed a relationship between variants in *COL5A1* and AD via targeted sequencing in 1.57% patients with sporadic aortic dissection. The *Col5a1* knockout rats exhibited AD after an intervention, indicating that *COL5A1* is a causative gene of AD. Activation of the transforming growth factor-β-signaling pathway may be implicated in the pathogenesis of this kind of AD.

Key Words: aortic dissection ■ *COL5A1* ■ targeted next-generation sequencing ■ TGF-β-signaling pathway

Aortic dissection (AD) is one of the most common deadly aortic diseases[1,2] and has ≈1/10 000 annual incidence in Europe.[3,4] Although AD is a catastrophic sudden cardiovascular disease with high mortality, it does not exhibit apparent manifestation until dissection emerges.[5,6] Since the first AD case in 1760, many studies have investigated the risk factors for AD including smoking and genetic disorders.[4,7,8]

The large-scale genome-wide association studies have been unsuccessfully applied in identifying a specific causative gene for AD. However, high throughput next-generation sequencing has shown promising breakthrough in identifying pathogenic genes in patients with AD.[9–11] It has been revealed that >25% of patients with AD exhibit the underlying pathogenic variants of AD causative gene before its onset.[12] Among the patients with AD, syndromic diseases is one of the major causes that accounts for >10% of cases.[13] To date, at least 13 causative genes (*TGFB2*, *TGFB3*, *TGFBR1*, *TGFBR2*, *SMAD3*, *SLC2A10*, *PLOD1*, *NOTCH1*, *MYLK*, *MYH11*, *FBN1*, *COL3A1*, and *ACTA2*) have been identified to cause AD in syndromic disease. These syndromic diseases include Marfan syndrome, Loeys-Dietz syndrome,

Correspondence to: Dao Wen Wang, MD, PhD, Division of Cardiology, Department of Internal Medicine, Tongji Hospital, Tongji Medical College, Huazhong University of Science and Technology, 1095# Jiefang Ave, Wuhan 430030, China. E-mail: dwwang@tjh.tjmu.edu.cn

†P. Chen and B. Yu contributed equally.

Supplementary Material for this article is available at https://www.ahajournals.org/doi/suppl/10.1161/JAHA.120.019276

For Sources of Funding and Disclosures, see page 10.

JAHA is available at: www.ahajournals.org/journal/jaha

CLINICAL PERSPECTIVE

What Is New?

- This study demonstrates an association between the *COL5A1* gene and aortic dissection by next-generation sequencing in a large sample of subjects with sporadic aortic dissection and *Col5a1* knockout rats for the first time.

What Are the Clinical Implications?

- Activation of the transforming growth factor beta 1-signaling pathway is likely to contribute to the pathogenicity of this kind of aortic dissection, and these results provide further insight into the genetic origin and potential therapeutic targets of aortic dissection.

Nonstandard Abbreviations and Acronyms

AD	aortic dissection
AngII	angiotensin II
BAPN	β-aminopropionitrile monofumarate
COL5A1	collagen type V alpha 1 chain
EDS	Ehlers-Danlos syndrome
MMP9	matrix metallopeptidase 9
α-SMA	alpha-smooth muscle actin
SMAD2	SMAD family member 2
SMC	smooth muscle cell
TGF-β1	transforming growth factor beta 1
WT	wild type

vascular Ehlers-Danlos syndrome (EDS), bicuspid aortic valve, and familial thoracic aortic aneurysm and dissection syndrome.[14–16]

The classic type of EDS is a rare autosomal dominant disease caused by a mutation in *COL5A1* and *COL5A2*. The disease is characterized by fragile, hyperextensible skin, hypermobile joints, and poor wound healing. Different from the vascular form of EDS, vascular lesions including aneurysms and dissections do not usually manifest in classic EDS.[17] In 2018, a study reported that the knockout of *Col5a2* in mice resulted in aortic aneurysms and dissections.[18] Furthermore, recent studies have reported some instances where patients with iliac or renal artery dissection carry *COL5A1* variants.[19–21] However, the AD phenotype has not been observed in patients harboring *COL5A1* variants.

To date, whether variants in *COL5A1* and *COL5A2* can cause AD is still unclear. Here, we investigate whether variants in the *COL5A1* gene are the genetic cause of AD in 702 patients with sporadic AD and *Col5a1* knockout rats.

METHODS

The data that support the findings of this study are available from the corresponding author upon reasonable request.

Participants Enrollment

We enrolled 702 consecutive unrelated patients with sporadic AD and 163 ethnically and age-matched controls with Han Chinese ancestry. Study of patients was conducted at the Tongji Hospital in Wuhan during a time period spanning the month of May 2008 and the month of May 2015. The study was approved by the Ethics Committee of Tongji Hospital, Tongji Medical College, Huazhong University of Science and Technology. An informed consent was obtained from the participants. All recruited patients with AD were diagnosed by computed tomography or magnetic resonance imaging. All the healthy controls were randomly recruited from healthy individuals undergoing health examinations in Tongji Hospital. All healthy controls were evaluated to be free of AD by medical history, physical examinations, and aorta imaging examinations (computed tomography or magnetic resonance imaging).

Panel Construction and Targeted Sequencing

A next-generation sequencing panel, including 529.73 kb full coding regions of 152 vessel matrix-related genes, was designed to identify potential genetic causes of AD as previously described (Table S1).[22] Targeted sequencing was performed for all patients with AD and healthy controls according to the Ampliseq semiconductor next-generation sequencing platform (Ion Torrent, Thermo Fisher, Carlsbad, CA) as per our previous description.[23]

Bioinformatics Analysis

The raw data of the next-generation sequencing were first processed using Ion Torrent platform-specific software, Torrent Suite v5.0. The generated reads were then aligned to the hg19/GRCh37 human reference genome for call variants and coverage status analysis. Thereafter, all the variants were comprehensively annotated using the Ion Reporter software 5.0 (Thermo Fisher). Subsequently, the Human Gene Mutation Database and the ClinVar database were searched to identify pathogenic variants responsible for AD. The focus was mainly on rare potential pathogenic variants rather than common alleles with

modest disease liability. Therefore, common variants (minor allele frequency ≥0.01) reported in the 1000-Genomes-Project, the Genome Aggregation Database, the Exome Sequencing Project, and Exome Aggregation Consortium database were excluded. To predict the pathogenesis of nonsynonymous variants, all nonsynonymous variants were scored using Polymorphism Phenotyping v2, Sorting Intolerant from Tolerant, and Mutation Taster. A potential pathogenic variant was predicted to be damaging if reported by at least 2 prediction softwares. The degrees of evolutionary conservation across multiple species of the missense variants were estimated with the phyloP score. All putative pathogenic variants were presumed to be absent in all 163 healthy controls and were validated by Sanger sequencing. The optimal sequence kernel association test was used to evaluate the association between COL5A1 and AD risk.[24]

Sanger Sequencing Validation

Polymerase chain reaction amplification was performed using the Taq Hot Start version (TaKaRa, Japan) to eliminate false-positive variants detected by next-generation sequencing. Sanger sequencing was then performed for all putative pathogenic variants using the Big Dye v.1.1 terminator cycle sequencing kit and Applied Biosystems 3500xl capillary sequencer (Applied Biosystems, Foster City).

Animals

All animal care and investigation conformed to the *Guide for the Care and Use of Laboratory Animals* by the US National Institutes of Health (Publication No. 85-23, revised 1996). This study was reviewed and approved by the Institutional Animal Research Committee of Tongji Medical College. The *Col5a1-flox* (*Col5a1*$^{fl/fl}$) and transgenic cre SD rats were established via the CRISPR/Cas9 system in the Beijing Laboratory Animal Research Center of the Chinese Academy of Medical Sciences. *Col5a1*$^{fl/fl}$ rats were mated with the transgenic cre rats to create heterozygous *Col5a1* knockout (*Col5a1*$^{+/-}$) rats. All the experimental rats were housed at the animal care room at 25°C with 12/12 hour light/dark cycles. The rats were fed with a normal diet and adequate water during the investigation. The weight of each rat was recorded weekly. The genotypes of rats were identified using validation primers (Table S2).

Development of AD Rat Models

Col5a1$^{+/-}$ and *Col5a1*$^{fl/fl}$ SD rats aged 3 weeks (>8 rats in each group) were fed on water with low-dose β-aminopropionitrile monofumarate (BAPN) (Sigma-Aldrich, St. Louis, MO) added (0.1 g/kg per day) for 4 weeks.[25] Osmotic minipumps (Model 1003D; Alzet, Cupertino, CA) filled with 1 μg/kg per minute angiotensin II (AngII) (Sigma-Aldrich) were implanted subcutaneously into 7-week-old rats. The rats in the control subgroup were fed on a normal diet and water, followed by using osmotic minipumps filled with normal saline. Blood pressure measurements were taken before and after implantation using the tail-cuff method. The rats were euthanized 72 hours after the implantation. The aorta of each rat was isolated and photographed.

Histology and Immunofluorescence Analysis

The thoracic aorta and abdominal aorta tissues were harvested and cut into 4-μm-thick sections. The sections were fixed in 4% paraformaldehyde and embedded in paraffin. Hematoxylin and eosin staining, Masson's trichrome staining, and elastic Van Gieson staining were subsequently performed. In addition, the sections were immunostained with rabbit polyclonal antibody against alpha-smooth muscle actin (α-SMA) and mouse monoclonal antibody against elastin. The nucleus was stained using 2-(4-amidinophenyl)-6-indolecarbamidine dihydrochloride. The immunofluorescence images were observed via a laser confocal microscope (Olympus, FV500-IX71, Tokyo, Japan).

Electron Microscopy

Small parts of the aorta tissue samples were fixed using 2% glutaraldehyde in 0.1 mmol/L cacodylate buffer. After dehydrating and embedding, ultrathin sections were stained. Collagen and elastin were observed using the Tecnai G20 TWIN electron microscope in 10 randomly selected areas, and ultrastructure analyses were performed in 3 rats in each group.

Western Blot Analysis

Western blots were performed as previously described.[26] Briefly, the aorta tissues were homogenized in ice-cold lysis buffer, and centrifuged at 4°C 12 000*g* for 20 minutes. The lysates (25 μg protein per lane) were resolved by 10% SDS-PAGE and then transferred to polyvinylidine difluoride membranes (0.45 μm). The membranes were blocked with 3% BSA and 5% nonfat milk for 2 hours and then incubated overnight with primary antibodies at 4°C. Afterward, peroxidase-conjugated secondary antibodies were incubated with membranes for 2 hours. The Western blots were visualized with enhanced chemiluminescence.

Antibodies

Antibodies against collagen type V alpha 1 chain (COL5A1) (A1515), SMAD family member 2 (SMAD2) (A11498), phosphorylation SMAD family member 2 (AP0269), and elastin (A2723) were acquired from ABclonal (Wuhan, China); antibodies against matrix metallopeptidase 9 (MMP9) (10375-2-AP), transforming growth factor-beta 1 (TGF-β1) (21898-1-AP), GAPDH (10494-1-AP), and α-SMA (55135-1-AP) were obtained from Proteintech (Wuhan, China); elastin (sc-166543) was obtained from Santa Cruz Biotechnology (CA); secondary antibodies were acquired from Pierce Biotechnology (IL).

Statistical Analysis

Data are presented as mean±SD. The analyses of differences among the groups were performed using Student *t* test and 1-way ANOVA, which were corrected by Bonferroni correction. In small-sample group, permutation tests were used for correction. Statistical analysis was performed using SPSS software 20.0 and R (version 3.6.1, Vienna, Austria). The differences were considered to be statistically significant if 2-tailed $P<0.05$.

RESULTS

Baseline Characteristics

We studied the baseline characteristics of 702 patients with AD and 163 healthy controls. There were no significant differences between the 2 groups in terms of age (53.2±11.9 versus 54.5±11.4), proportion of men (78.1% versus 78.5%), proportion of hypertension (54.1% versus 54.8%), and proportion of smokers (45.6% versus 46.1%). These outcomes were consistent with our previous study results.[22]

Next-Generation Sequencing Quality

In the next-generation sequencing, the mean base coverage depth for 702 patients with AD and 163 health controls was more than 700-fold per sample. This was similar to our previous study.[22]

Targeted Next-Generation Sequencing Revealed That *COL5A1* was Associated With AD

Targeted next-generation sequencing was performed for 702 unrelated Han Chinese patients with AD and 163 matched healthy controls. A predefined AD panel including *COL5A1* was used to identify the pathogenic and likely pathogenic variants. As a result, 11 likely pathogenic variants in *COL5A1* were identified in 11 patients with AD (Table 1). All the 11 variants were novel missense variants that had not been reported in the genetic variant database. These variants in *COL5A1* accounted for 1.57% (11/702) of the AD cases. There were no potential pathogenic variants that were found in the healthy control group (0/163). The sequence

Table 1. Potential Pathogenic Variants in *COL5A1* Gene Identified in 702 Patients With AD

No. of Related Patients	Coding Change	Protein Change	SIFT (Score)	Polyphen-2 (Score)	Mutation Taster (Score)	PhyloP
1	c.487G>A	p. Gly163Ser	Damaging (0.002)	Probably damaging (1.000)	Disease causing (0.99999)	1.048
1	c.1372C>T	p. Pro458Ser	Damaging (0.032)	Probably damaging (1.000)	Disease causing (0.99999)	0.852
1	c.2768C>T	p. Pro923Leu	Tolerated (0.097)	Probably damaging (0.998)	Disease causing (0.99999)	0.786
1	c.2842C>T	p. Arg948Trp	Damaging (0.003)	Probably damaging (1.000)	Disease causing (0.99985)	0.883
1	c.3292G>A	p. Ala1098Thr	Damaging (0.022)	Probably damaging (1.000)	Disease causing (0.99999)	1.038
1	c.3398G>A	p. Arg1133Gln	Damaging (0.041)	Probably damaging (0.997)	Disease causing (0.99999)	0.943
1	c.3431G>C	p. Gly1144Ala	Damaging (0.000)	Probably damaging (0.999)	Disease causing (0.99999)	0.943
1	c.3445G>A	p. Val1149Met	Tolerated (1.000)	Probably damaging (0.978)	Disease causing (0.96904)	0.952
1	c.3752C>T	p. Pro1251Leu	Tolerated (0.130)	Probably damaging (1.000)	Disease causing (0.99999)	0.843
1	c.4241G>C	p. Gly1414Ala	Damaging (0.000)	Probably damaging (0.954)	Disease causing (0.99999)	1.026
1	c.5263G>A	p. Ala1755Thr	Tolerated (0.565)	Probably damaging (0.910)	Disease causing (0.75559)	0.953

RefSeq: NM_000093.4.
AD indicates aortic dissection; PhyloP, phylogenetic P-values.

kernel association test performed on the *COL5A1* gene between the 2 groups revealed that the likely pathogenic variants in the COL5A1 gene were significantly enriched in patients with AD (P=0.0037), thus suggesting that variants in *COL5A1* were associated with AD.

Correlation Between Genotype and Phenotype

In patients with AD carrying variants in *COL5A1*, the mean age of AD onset was 59.9 years old, significantly higher than the mean onset age of all patients with AD (53.2 years). Meanwhile, the percentage of smokers (63.6% versus 45.6%, P=0.612), hypertensives (72.7% versus 54.1%, P=0.219), and DeBakey Type 3 AD (mild type of AD) (81.8% versus 75.2%, P=0.614) in *COL5A1* carried patients were higher compared with the total AD cohort, though there were no statistically significant differences (Table 2).

Generation of *Col5a1* Knockout Rat Model

Col5a1 knockout rats were established to validate the hypothesis of a relationship between the *Col5a1* gene and AD. The *Col5a1*$^{fl/fl}$ rats were generated using the CRISPR/Cas9 system by inserting a loxP sequence into intron 1 and intron 2. After mating the *Col5a1*$^{fl/fl}$ and transgenic cre rats, 214 bp bases including exon 2 were deleted, generating a new termination codon in exon 3 (Figure S1). Consequently, all the critical domains of the *Col5a1* gene were truncated (Figure 1A), and *Col5a1* knockout (*Col5a1*$^{+/-}$) rats were obtained. The genotypes of the rats were identified using polymerase chain reaction amplification and Sanger sequencing (Figure 1B, Figure S2). Meanwhile, the COL5A1 protein levels in different genotype rats were examined using Western blotting. The results revealed that protein levels of COL5A1 in *Col5a1*$^{+/-}$ rats were significantly lower than in *Col5a1*$^{fl/fl}$ rats (Figure 1C). These results indicate that the *Col5a1* knockout rats were successfully generated.

Col5a1 Knockout Rats Exhibited Collagen and Elastin Disarray Ultrastructure

Littermate controls were generated by mating *Col5a1*$^{+/-}$ rats. The birth sex ratio of the wild type (WT) to *Col5a1*$^{+/-}$ rats was ≈1:2. However, no *Col5a1*$^{-/-}$ rats were obtained during the entire study, indicating homozygous knockout of *Col5a1* can cause embryonic death (Table S3). This is consistent with our previous research.[27] The body weight of *Col5a1*$^{+/-}$ rats from 4 to 9 weeks postbirth was significantly lower than WT rats, indicating that heterozygous knockout of *Col5a1* affects the growth of *Col5a1*$^{+/-}$ rats (Table S3, Figure S3). There were no significant differences found in the noninvasive systolic and diastolic blood pressure between the 2 groups (Table S3). Thus, knockout of *Col5a1* does not affect the baseline blood pressure of the rats. There was no significant difference in the percentage of survival in 48 weeks between the 2 groups (Figure 1D). Rats in the *Col5a1*$^{+/-}$ group exhibited scoliosis, while this phenotype was not found in the WT group (Figure 1E). Notably, no AD phenotype or aortic aneurysm was found in 6-week-old rats in either the WT group or the *Col5a1*$^{+/-}$ group (Figure 1F). Moreover, no significant structural abnormality or fibrils disarray was found in hematoxylin and eosin, Masson, and elastic Van Gieson staining (Figure 1G). In elderly rats (48 week-old) in the WT or *Col5a1*$^{+/-}$ groups, either significant aortic lesion or structure abnormality was not found. The ultrastructural structure of aorta was observed using electron microscopy, and 10 random microscopic fields were selected in each sample. The fracture of elastic fibers and disarray of collagenous fibers was observed in 6-week-old rats in

Table 2. Clinical Characteristics and Genotypes of the Patients Carrying Potential Pathogenic Variants in *COL5A1* Gene

Gene	Genotype	Age, y	Sex	History of Smoking	Medical History of Hypertension	DeBakey Type of AD
COL5A1	c.487G>A	46	Female	No	Yes	3
COL5A1	c.1372C>T	68	Male	No	Yes	3
COL5A1	c.2768C>T	54	Male	Yes	No	3
COL5A1	c.2842C>T	36	Male	No	Yes	3
COL5A1	c.3292G>A	65	Male	Yes	No	3
COL5A1	c.3398G>A	60	Male	Yes	No	1
COL5A1	c.3431G>C	71	Male	Yes	Yes	3
COL5A1	c.3445G>A	59	Male	No	Yes	1
COL5A1	c.3752C>T	86	Male	Yes	Yes	3
COL5A1	c.4241G>C	58	Male	Yes	Yes	3
COL5A1	c.5263G>A	56	Male	Yes	Yes	3

RefSeq: NM_000093.4.
AD indicates aortic dissection.

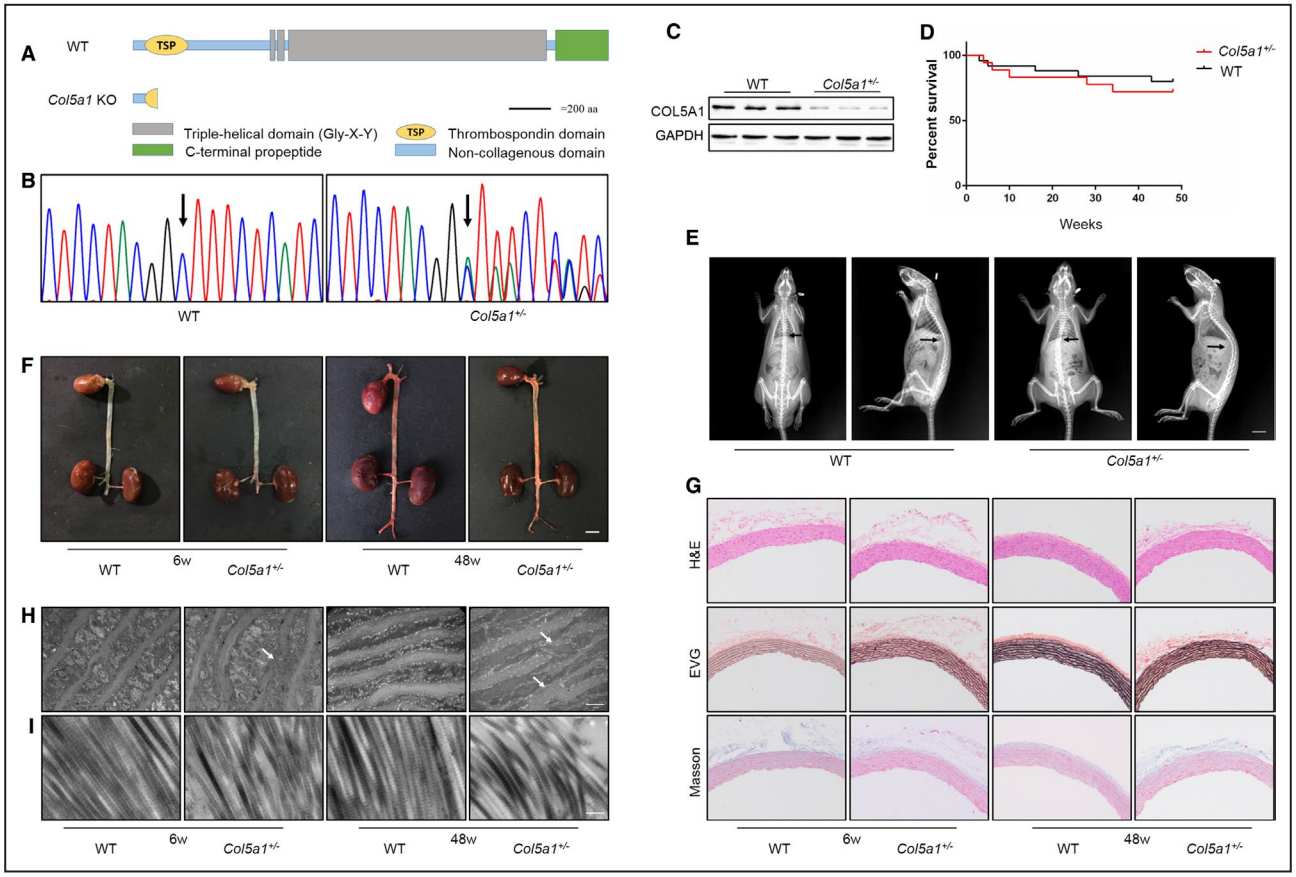

Figure 1. *Col5a1* KO rat revealed fracture in elastic fibers and disarray in collagenous fibers.
A, The mode of *Col5a1* KO compared with that of the WT. **B**, Identification of littermate control rats via Sanger sequencing. **C**, Western blot demonstrated that protein levels of *COL5A1* decreased in *Col5a1*$^{+/-}$ rats, indicating that the *Col5a1* KO model was successfully established. **D**, The percentage of survival in 48 wks showed that there was no significant difference between WT (n=25) and *Col5a1*$^{+/-}$ rats (n=20). **E**, The *Col5a1*$^{+/-}$ group rats exhibited scoliosis, but was not found in the WT group. Scale bar: 1 cm. **F**, Aortic dissection phenotype was found in 6-wk-old rats in either WT group or *Col5a1*$^{+/-}$ group. Scale bar: 1 cm. **G**, No significant structural abnormality or fibril disarray was observed from H&E, Masson, and EVG staining. Scale bar: 100 μm. **H**, Electron microscopy showed fracture of elastic fibers in the aorta of 6-wk-old *Col5a1*$^{+/-}$ rats and this was more severe in 48-week-old *Col5a1*$^{+/-}$ rats. The white arrows indicate elastic fibers fracture. Scale bar: 1 μm. **I**, Electron microscopy revealed a disarray of collagenous fibers in the aorta of 6-wk-old *Col5a1*$^{+/-}$rats, and the disarray was more severe in 48-wk-old *Col5a1*$^{+/-}$ rats. Scale bar: 1 μm. *Col5a1* indicates collagen type V alpha 1 chain; EVG, elastic Van Gieson; H&E, hematoxylin and eosin; KO, knockout; and WT, wild type.

the *Col5a1*$^{+/-}$ group, but not in the WT group (93.3% versus 0.0%, P<0.001). The structural damages in elastic and collagenous fibers were more severe in 48-week-old rats in the *Col5a1*$^{+/-}$ group (Figure 1H and 1I). Although *Col5a1*$^{+/-}$ rats did not exhibit the phenotype of AD or aortic aneurysm, the results still revealed that knockout of *the Col5a1* gene caused fibrils fracture in the ultrastructural structure.

Col5a1 Knockout Predisposed Rat AD Model to High AD Incidence

To further validate the association between *COL5A1* and AD, we used BAPN and AngII to induce AD in rats. Noninvasive systolic and diastolic blood pressure increased significantly in both groups after using AngII, and there were no significant differences between the 2 groups (Figure S4). After the rats were fed on BAPN for 4 weeks, 37.5% of the rats revealed microaneurysm in the *Col5a1*$^{+/-}$ group, but not in the WT group (Figure 2A, 2B, and Figure S5). However, no AD or microaneurysm was observed in both groups after AngII implantation for 3 days. After the administration of BAPN+AngII, 70.0% of the rats exhibited AD in the *Col5a1*$^{+/-}$ group and only 8.3% of rats presented with AD in the WT group (Figure 2A and 2B). This indicates that *Col5a1* knockout rats were predisposed to a high incidence of AD. Compared with the WT group, the intervention of BAPN+AngII was associated with high mortality in the *Col5a1*$^{+/-}$ group in 72 hours (Figure 2C). Furthermore, after induced AD via BAPN and BAPN+AngII, histology analyses showed significant disarray of collagenous fibers, fracture of elastic fibers, and tears in the vessel wall in the *Col5a1*$^{+/-}$ group but not in the WT group

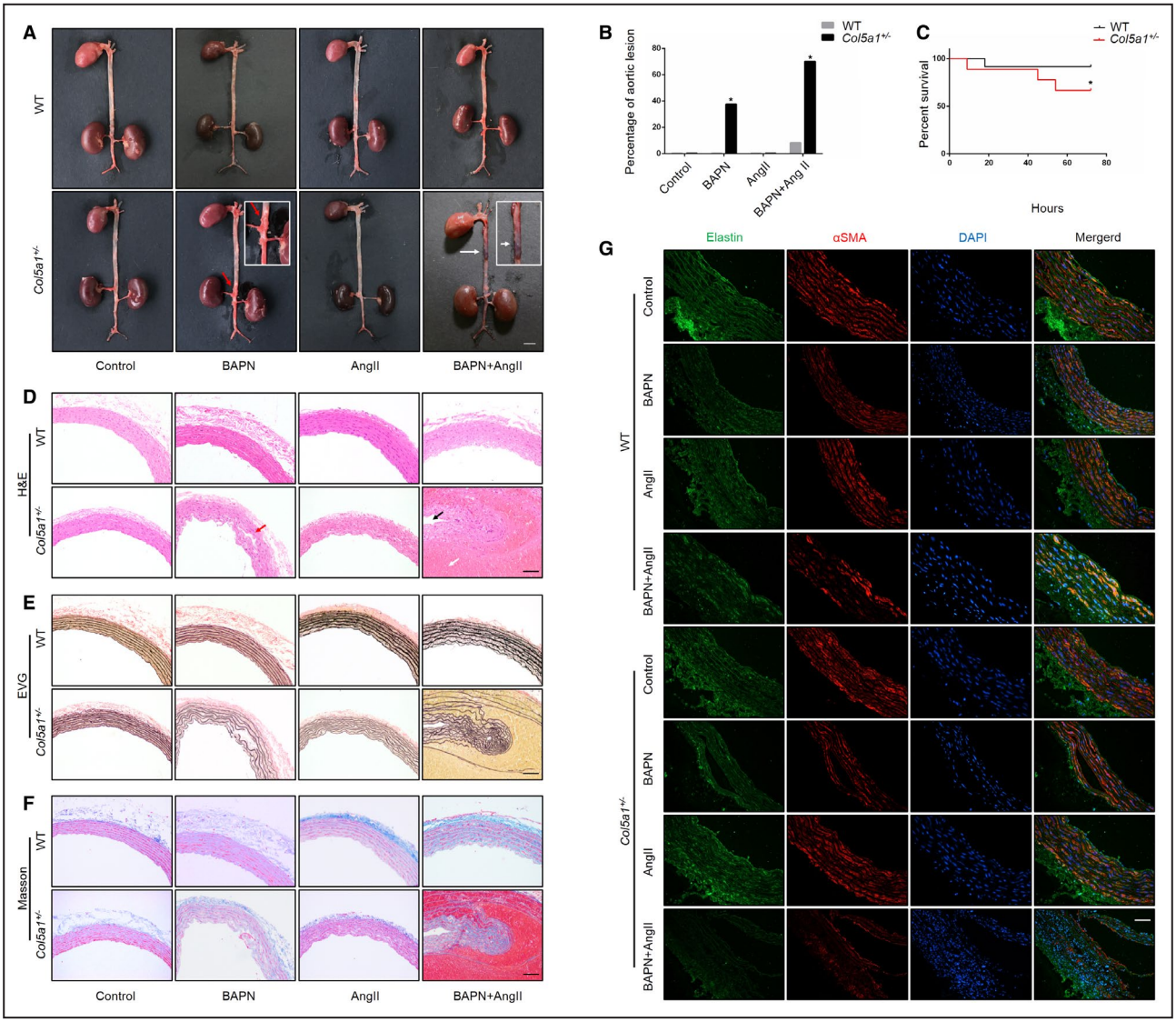

Figure 2. *Col5a1* knockout predisposed rat AD model to high AD incidence.
A, The *Col5a1*$^{+/-}$ rats presented with microaneurysm in BAPN subgroup and AD in BAPN+AngII subgroup. The red arrow indicates microaneurysm; the white arrow indicates AD. **B**, A significantly high percentage of aortic lesion in the *Col5a1*$^{+/-}$ group was found after the intervention. *P<0.05. **C**, Compared with the WT group, the intervention of BAPN+AngII was associated with high mortality in the *Col5a1*$^{+/-}$ group after 72 h. *P<0.05. **D**, H&E staining disclosed minor tears in the vascular wall and AD in the BAPN subgroup and the BAPN+AngII subgroup of *Col5a1*$^{+/-}$ rats, respectively. Scale bar: 200 μm. The red arrow indicates a fracture of elastic fibers; the white arrow indicates the false aorta lumen; the black arrow indicates the original aorta lumen. **E**, EVG staining indicated a fracture of the elastic fibers in *Col5a1*$^{+/-}$ rats. Scale bar: 200 μm. **F**, Masson staining revealed a disarray of collagenous fibers in *Col5a1*$^{+/-}$ rats. Scale bar: 200 μm. **G**, Immunofluorescence indicated disarray and reduced expression of elastic fibers and αSMA in *Col5a1*$^{+/-}$ rats treated with BAPN alone as well as BAPN+AngII. Scale bar: 200 μm. AD indicates aortic dissection; AngII, angiotensin II; BAPN, β-aminopropionitrile monofumarate; *Col5a1*, collagen type V alpha 1 chain; DAPI, 2-(4-amidinophenyl)-6-indolecarbamidine dihydrochloride; EVG, elastic Van Gieson; H&E, hematoxylin and eosin; αSMA, alpha smooth muscle actin; and WT, wild type.

(Figure 2D through 2F). The immunofluorescence results revealed that there was disarray and reduced expression of elastic fibers and αSMA was observed in the *Col5a1*$^{+/-}$ group compared with the WT group after administering BAPN and BAPN+AngII (Figure 2G). These results confirmed that *Col5a1* knockout was associated with high AD morbidity in the stress model compared with WT rats.

Col5a1 Knockout Triggered AD by Activating the TGF-β-Signaling Pathway

The TGF-β signaling pathway is an important signaling pathway associated with the pathogenesis of AD. A previous study reported that the TGF-β-signaling pathway was activated in patients with AD.[28,29] Western blot analysis of the aorta samples showed that the level of TGF-β1 was higher in the *Col5a1*$^{+/-}$ group than in

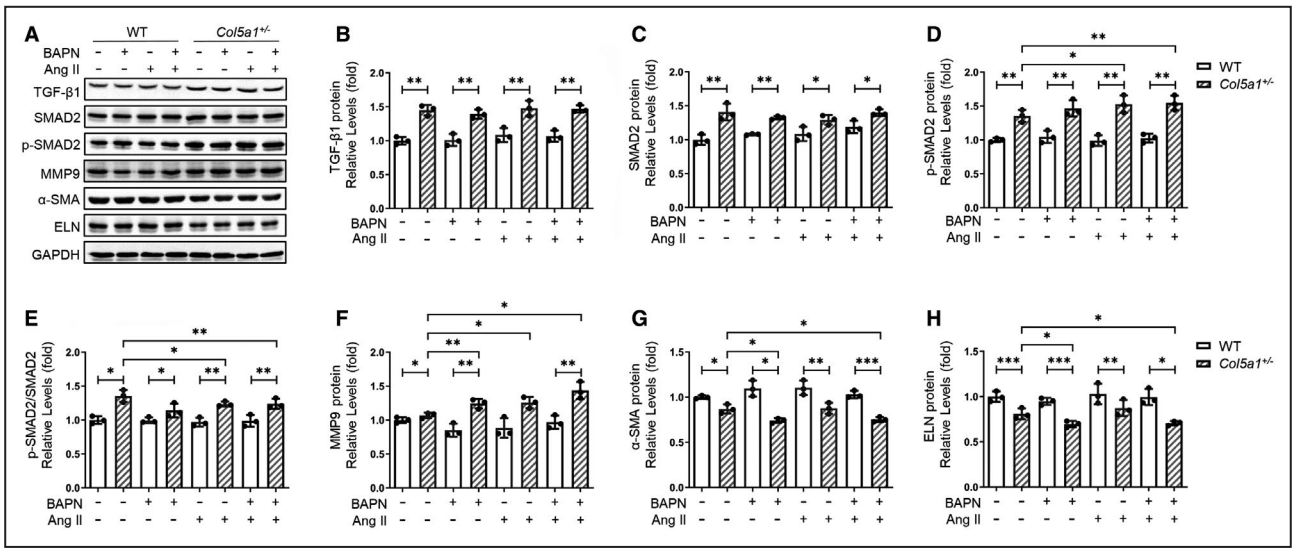

Figure 3. *Col5a1* knockout activated TGF-β-signaling pathway.
A, Western blotting of TGF-β1, SMAD2, p-SMAD2, MMP9, αSMA, and ELN in the aorta. **B**, TGF-β1 levels were higher in *Col5a1*$^{+/-}$ group than the WT group. **C**, SMAD2 was significantly elevated in the *Col5a1*$^{+/-}$ group. **D**, p-SMAD2 was significantly elevated in the *Col5a1*$^{+/-}$ group. The expression levels of p-SMAD2 in AngII and BAPN+AngII subgroups in *Col5a1*$^{+/-}$ rats were higher than in the control subgroup. **E**, The ratio of p-SMAD2/SMAD2 levels was significantly elevated in the *Col5a1*$^{+/-}$ group. The ratio of p-SMAD2/SMAD2 in AngII and BAPN+AngII subgroups in *Col5a1*$^{+/-}$ rats was higher than in the control subgroup. **F**, *Col5a1* knockout led to elevated expression of MMP9. The levels of MMP9 in *Col5a1*$^{+/-}$ rats after intervention were significantly higher than in the control subgroup. **G**, The expression of αSMA decreased significantly in the *Col5a1*$^{+/-}$ group. The expression of αSMA in AngII and BAPN+AngII subgroups in *Col5a1*$^{+/-}$ rats decreased significantly. **H**, ELN expression was significantly decreased in the *Col5a1*$^{+/-}$ group. The expression level of ELN in AngII and BAPN+AngII subgroups in *Col5a1*$^{+/-}$ rats was significantly lower than in the control subgroup. *indicates that $P<0.05$, **indicates that $P<0.01$, and ***indicates that $P<0.001$. AngII indicates angiotensin II; BAPN, β-aminopropionitrile monofumarate; *Col5a1*, collagen type V alpha 1 chain; ELN, elastin; MMP9, matrix metallopeptidase 9; p-SMAD2, phosphorylation SMAD family member 2; α-SMA, alpha smooth muscle actin; SMAD2, SMAD family member 2; TGF-β1, transforming growth factor beta 1; and WT, wild type.

the WT group (Figure 3A and 3B). Meanwhile, phosphorylation SMAD family member 2, total SMAD2, and the ratio of phosphorylation SMAD family member 2/SMAD2 increased significantly in the *Col5a1*$^{+/-}$ group. Moreover, in the *Col5a1*$^{+/-}$ group, the ratio of phosphorylation SMAD family member 2/SMAD2 was higher in AngII and BAPN+AngII subgroups than in the control subgroup (Figure 3A, 3C, 3D, and 3E). MMP is a protein that maintains the homeostasis of the vascular matrix.[30] Previous studies have reported that the expression of MMP9 increases once the TGF-β-signaling pathway is activated, subsequently affecting the smooth muscle cell (SMC) elastin-contractile units composite of elastin and SMCs.[31,32] Accordingly, the expression levels of MMP9 were significantly elevated in the *Col5a1*$^{+/-}$ group compared with the WT group. These levels were significantly higher in the intervention subgroups than in the control subgroup in the *Col5a1*$^{+/-}$ rats (Figure 3A and 3F). In addition, the levels of α-SMA and elastin were significantly reduced in the *Col5a1*$^{+/-}$ group. In the *Col5a1*$^{+/-}$ group, the α-SMA and elastin protein levels were reduced in BAPN and BANP+AngII subgroups compared with the control subgroup (Figure 3A, 3G, and 3H). Overall, these results suggest that *Col5a1* knockout partially causes AD by activating the TGF-β-signaling pathway.

DISCUSSION

The targeted sequencing completed in samples in 702 patients with sporadic AD in our previous study suggested that variants in *COL5A1* might be related to AD.[22] Accordingly, further analyses were performed in this study to identify these variants. A total of 11 likely pathogenic variants were identified in the *COL5A1* gene from 11 patients. These variants accounted for 1.57% of the AD cases studied and indicated that *COL5A1* is associated with AD. To further investigate the relationship between the *COL5A1* gene and AD, a *Col5a1* knockout rat model was established via the CRISPR/Cas9 system. Although no spontaneous AD or aortic aneurysm was found without intervention, fracture of elastic fibers and disarray of collagenous fibers were observed from electron microscopy in 6-week-old *Col5a1*$^{+/-}$ rats. Furthermore, in the rat AD model, *Col5a1* knockout rats were predisposed to higher AD incidence and mortality compared with WT rats. These results validated our hypothesis that

COL5A1 causes AD. Finally, subsequent mechanism analysis revealed that *Col5a1* knockout partially caused AD by activating the TGF-β-signaling pathway. In summary, these results suggest that variants in *COL5A1* trigger AD in the stress model via TGF-β-signaling pathway activation.

The majority of heritable AD with syndromic disease features can be attributed to mutations in the currently known causative genes. However, only 30% of heritable AD without syndromic disease features have mutations in these genes; thus more AD causative genes are unidentified.[14] The rare and highly penetrant genetic variants for AD are easy to recognize, but there are still a few penetrant variants that can increase the risk of AD only in combination with environmental risk factors or with a second low-risk variant.[14] Here, 11 patients with AD carrying potential pathogenic variants in *COL5A1* were identified. All the patients had either a medical history of hypertension or a history of smoking besides carrying the variants. Compared with all patients with AD recruited in this study, these 11 patients had an older mean age of onset, a higher percentage of hypertension, smoking, and DeBakey Type 3 AD. This is an indication that *COL5A1* is a modest AD causative gene with low penetrance. These results confirmed why the *Col5a1* knockout rats exhibit AD only after drug intervention.

Previous study revealed that at least 25% of AD is caused by genetic factors, and have a potential pathogenic mutation in at least 1 specific gene.[12] However, up to 80% of patients with AD are nonsyndromic and sporadic, which makes it more difficult to assess the genetic risk factors in these populations.[13] In this study, we revealed 1.57% of patients with AD carrying potential pathogenic variants in *COL5A1* gene, and we have identified other pathogenic genes that might be associated with sporadic AD using targeted next-generation sequencing in previous studies.[22,33] However, targeted sequencing is limited in terms of understanding the full spectrum of AD; thus whole exome sequencing or whole genome sequencing should be performed in the future.

Previous studies have reported that Col5a1$^{-/-}$ mice at the embryonic stage died because of the absence of collagen fibril formation.[27] In this study, homozygous embryonic death was found in *Col5a1* knockout rats. Meanwhile, all the *COL5A1* variants carried by the patients were found to be heterozygous, which is consistent with the phenomenon detected in rats.

COL5A1 is a causative gene of the classical EDS, and variants in *COL5A1* have been linked with scoliosis in some reported cases.[34,35] However, the scoliosis phenotype was only found in *Col5a1* knockout rats rather than patients with AD carrying *COL5A1* variants. This may be because null variants of *COL5A1* are the major type of mutation in classic EDS.[36] Thus, patients carrying missense variants do not exhibit syndromic features of classic EDS.

Earlier studies reported that activation of the TGF-β-signaling pathway is implicated in the production of vascular matrix proteins, leading to vascular remodeling.[37,38] In addition, the SMAD signaling pathway can be activated in the extracellular matrix mediated by TGF-β.[39] The TGF-β1/SMAD signaling pathway was found to be significantly activated in patients with AD,[28,29] consistent with findings of this study. Furthermore, TGF-β1 highly enhances the secretion of MMP9. The MMP9 was reported to be implicated in the pathogenesis of AD in human and animal models.[32,40,41] MMP9 activates elastin degradation and affects the function of SMC elastin-contractile units. The SMC elastin-contractile units are important for maintaining the structural integrity of the aorta, and loss of these units is involved in the pathological process of AD.[31,42,43] In this study, the level of MMP9 was significantly increased in the *Col5a1*$^{+/-}$ group, and disarray and reduced expression of elastin and α-SMA were observed in the *Col5a1*$^{+/-}$ group after intervention, thus indicating the functional SMC elastin-contractile units were reduced by elevated MMP9.

Previous studies demonstrated that angiotensin-converting enzyme (ACE) inhibitors are considered to be protective against AD or aortic aneurysm phenotype.[44,45] However, it is still unclear whether the ACE inhibitor could have benefits in patients with sporadic AD. In our study, a total of 11 patients were identified carrying potential pathogenic variants in COL5A1. According to 5-year follow-up data, 7 patients were using ACE inhibitors, and no death or recurrence of AD occurred in these patients, while recurrence of AD occurred in 1 patient without using an ACE inhibitor (0.0% versus 25%, P=0.417). More studies will be done to investigate whether ACE inhibitors could protect against AD in the future.

After targeted sequencing in 702 patients with AD and 163 controls, potentially pathogenic variants in *COL5A1* were found significantly enriched in the patients with AD group. Since the control group did not include a high number of participants, more cases and controls are needed in further studies. In addition, although it was found that *Col5a1* knockout can cause AD in the stress model partly by activating the TGF-β-signaling pathway, these data are still preliminary in delineating the causal relationship between TGF-β-signaling pathway and AD. More mechanism studies should be performed to investigate the role of other mechanisms in the pathogenesis of AD resulting from *Col5a1* knockout.

In conclusion, we demonstrate that variants in *COL5A1* are responsible for AD through targeted sequencing. Furthermore, it was confirmed that *Col5a1* knockout rats predisposed the rat AD model to high

AD incidence. Subsequently, mechanism analysis revealed that activation of the TGF-β-signaling pathway was partially implicated in AD pathogenesis. This study provides more insight into the genetic cause of AD.

ARTICLE INFORMATION

Received September 4, 2020; accepted March 29, 2021.

Affiliations

Division of Cardiology, Departments of Internal Medicine and Genetic Diagnosis Center, Tongji Hospital, Tongji Medical College, Huazhong University of Science and Technology, Wuhan, China (P.C., B.Y., Z.L., Y.C., Y.S., D.W.W.); Hubei Key Laboratory of Genetics and Molecular Mechanism of Cardiological Disorders, Wuhan, China (P.C., B.Y., Z.L., Y.C., Y.S., D.W.W.); and Collaborative Innovation Center for Genetics and Development, School of Life Sciences, Fudan University, Shanghai, China (D.W.W.).

Acknowledgments

The authors are grateful for all the participants in this study.

Sources of Funding

This study was supported by National Natural Science Foundation of China projects (No. 91839302) and National Key Research and Development Program of China (No. 2017YFC0909401).

Disclosures

None.

Supplementary Material

Tables S1–S3
Figures S1–S5

REFERENCES

1. Braverman AC. Acute aortic dissection: clinician update. *Circulation*. 2010;122:184–188. DOI: 10.1161/CIRCULATIONAHA.110.958975.
2. Núñez-Gil IJ, Bautista D, Cerrato E, Salinas P, Varbella F, Omedè P, Ugo F, Ielasi A, Giammaria M, Moreno R, et al. Incidence, management, and immediate- and long-term outcomes after iatrogenic aortic dissection during diagnostic or interventional coronary procedures. *Circulation*. 2015;131:2114–2119. DOI: 10.1161/CIRCULATIONAHA.115.015334.
3. Olsson C, Thelin S, Stahle E, Ekbom A, Granath F. Thoracic aortic aneurysm and dissection: increasing prevalence and improved outcomes reported in a nationwide population-based study of more than 14,000 cases from 1987 to 2002. *Circulation*. 2006;114:2611–2618. DOI: 10.1161/CIRCULATIONAHA.106.630400.
4. Goldfinger JZ, Halperin JL, Marin ML, Stewart AS, Eagle KA, Fuster V. Thoracic aortic aneurysm and dissection. *J Am Coll Cardiol*. 2014;64:1725–1739. DOI: 10.1016/j.jacc.2014.08.025.
5. Prakash SK, Haden-Pinneri K, Milewicz DM. Susceptibility to acute thoracic aortic dissections in patients dying outside the hospital: an autopsy study. *Am Heart J*. 2011;162:474–479. DOI: 10.1016/j.ahj.2011.06.020.
6. Sakai H, Suzuki S, Mizuguchi T, Imoto K, Yamashita Y, Doi H, Kikuchi M, Tsurusaki Y, Saitsu H, Miyake N, et al. Rapid detection of gene mutations responsible for non-syndromic aortic aneurysm and dissection using two different methods: resequencing microarray technology and next-generation sequencing. *Hum Genet*. 2012;131:591–599. DOI: 10.1007/s00439-011-1105-7.
7. Criado FJ. Aortic dissection: a 250-year perspective. *Tex Heart Inst J*. 2011;38:694–700.
8. Rampoldi V, Trimarchi S, Eagle KA, Nienaber CA, Oh JK, Bossone E, Myrmel T, Sangiorgi GM, De Vincentiis C, Cooper JV, et al. Simple risk models to predict surgical mortality in acute type A aortic dissection: the International Registry of Acute Aortic Dissection score. *Ann Thorac Surg*. 2007;83:55–61. DOI: 10.1016/j.athoracsur.2006.08.007.
9. Manolio TA, Collins FS, Cox NJ, Goldstein DB, Hindorff LA, Hunter DJ, McCarthy MI, Ramos EM, Cardon LR, Chakravarti A, et al. Finding the missing heritability of complex diseases. *Nature*. 2009;461:747–753. DOI: 10.1038/nature08494.
10. LeMaire SA, McDonald M-L, Guo D-C, Russell L, Miller CC III, Johnson RJ, Bekheirnia MR, Franco LM, Nguyen M, Pyeritz RE, et al. Genome-wide association study identifies a susceptibility locus for thoracic aortic aneurysms and aortic dissections spanning FBN1 at 15q21.1. *Nat Genet*. 2011;43:996–1000. DOI: 10.1038/ng.934.
11. Marian AJ, Belmont J. Strategic approaches to unraveling genetic causes of cardiovascular diseases. *Circ Res*. 2011;108:1252–1269. DOI: 10.1161/CIRCRESAHA.110.236067.
12. Milewicz D, Hostetler E, Wallace S, Mellor-Crummey L, Gong L, Pannu H, Guo DC, Regalado E. Precision medical and surgical management for thoracic aortic aneurysms and acute aortic dissections based on the causative mutant gene. *J Cardiovasc Surg (Torino)*. 2016;57:172–177.
13. Campens L, Callewaert B, Muino Mosquera L, Renard M, Symoens S, De Paepe A, Coucke P, De Backer J. Gene panel sequencing in heritable thoracic aortic disorders and related entities—results of comprehensive testing in a cohort of 264 patients. *Orphanet J Rare Dis*. 2015;10:9. DOI: 10.1186/s13023-014-0221-6.
14. Pinard A, Jones GT, Milewicz DM. Genetics of thoracic and abdominal aortic diseases. *Circ Res*. 2019;124:588–606. DOI: 10.1161/CIRCRESAHA.118.312436.
15. Hoffjan S. Genetic dissection of Marfan syndrome and related connective tissue disorders: an update 2012. *Mol Syndromol*. 2012;3:47–58. DOI: 10.1159/000339441.
16. Khau Van Kien P, Wolf J-E, Mathieu F, Zhu L, Salve N, Lalande A, Bonnet C, Lesca G, Plauchu H, Dellinger A, et al. Familial thoracic aortic aneurysm/dissection with patent ductus arteriosus: genetic arguments for a particular pathophysiological entity. *Eur J Hum Genet*. 2004;12:173–180. DOI: 10.1038/sj.ejhg.5201119.
17. Ritelli M, Dordoni C, Venturini M, Chiarelli N, Quinzani S, Traversa M, Zoppi N, Vascellaro A, Wischmeijer A, Manfredini E, et al. Clinical and molecular characterization of 40 patients with classic Ehlers-Danlos syndrome: identification of 18 COL5A1 and 2 COL5A2 novel mutations. *Orphanet J Rare Dis*. 2013;8:58. DOI: 10.1186/1750-1172-8-58.
18. Park AC, Phan N, Massoudi D, Liu Z, Kernien JF, Adams SM, Davidson JM, Birk DE, Liu B, Greenspan DS. Deficits in Col5a2 expression result in novel skin and adipose abnormalities and predisposition to aortic aneurysms and dissections. *Am J Pathol*. 2017;187:2300–2311. DOI: 10.1016/j.ajpath.2017.06.006.
19. Borck G, Beighton P, Wilhelm C, Kohlhase J, Kubisch C. Arterial rupture in classic Ehlers-Danlos syndrome with COL5A1 mutation. *Am J Med Genet A*. 2010;152A:2090–2093. DOI: 10.1002/ajmg.a.33541.
20. Mehta S, Dhar SU, Birnbaum Y. Common iliac artery aneurysm and spontaneous dissection with contralateral iatrogenic common iliac artery dissection in classic Ehlers-Danlos syndrome. *Int J Angiol*. 2012;21:167–170. DOI: 10.1055/s-0032-1325118.
21. Monroe GR, Harakalova M, van der Crabben SN, Majoor-Krakauer D, Bertoli-Avella AM, Moll FL, Oranen BI, Dooijes D, Vink A, Knoers NV, et al. Familial Ehlers-Danlos syndrome with lethal arterial events caused by a mutation in COL5A1. *Am J Med Genet A*. 2015;167:1196–1203.
22. Li Z, Zhou C, Tan L, Chen P, Cao Y, Li X, Yan J, Zeng H, Wang DW, Wang DW. A targeted sequencing approach to find novel pathogenic genes associated with sporadic aortic dissection. *Sci China Life Sci*. 2018;61:1545–1553. DOI: 10.1007/s11427-018-9382-0.
23. Li Z, Huang J, Zhao J, Chen C, Wang H, Ding H, Wang DW, Wang DW. Rapid molecular genetic diagnosis of hypertrophic cardiomyopathy by semiconductor sequencing. *J Transl Med*. 2014;12:173. DOI: 10.1186/1479-5876-12-173.
24. Lee S, Emond MJ, Bamshad MJ, Barnes KC, Rieder MJ, Nickerson DA; Team NGESP-ELP, Christiani DC, Wurfel MM, Lin X. Optimal unified approach for rare-variant association testing with application to small-sample case-control whole-exome sequencing studies. *Am J Hum Genet*. 2012;91:224–237. DOI: 10.1016/j.ajhg.2012.06.007.
25. Nagashima H, Uto K, Sakomura Y, Aoka Y, Sakuta A, Aomi S, Hagiwara N, Kawana M, Kasanuki H. An angiotensin-converting enzyme inhibitor, not an angiotensin II type-1 receptor blocker, prevents beta-aminopropionitrile monofumarate-induced aortic dissection in rats. *J Vasc Surg*. 2002;36:818–823.
26. Li H, Zhang X, Wang F, Zhou L, Yin Z, Fan J, Nie X, Wang P, Fu X-D, Chen C, et al. MicroRNA-21 lowers blood pressure in spontaneous hypertensive rats by upregulating mitochondrial translation. *Circulation*. 2016;134:734–751. DOI: 10.1161/CIRCULATIONAHA.116.023926.
27. Wenstrup RJ, Florer JB, Brunskill EW, Bell SM, Chervoneva I, Birk DE. Type V collagen controls the initiation of collagen fibril assembly. *J Biol Chem*. 2004;279:53331–53337. DOI: 10.1074/jbc.M409622200.

28. Yuan SM, Lin H. Expressions of transforming growth factor beta1 signaling cytokines in aortic dissection. *Braz J Cardiovasc Surg*. 2018;33:597–602.
29. Yuan SM. Transforming growth factor beta1/Smad signalling pathway of aortic disorders: histopathological and immunohistochemical studies. *Folia Morphol*. 2012;71:31–38.
30. Barbour JR, Spinale FG, Ikonomidis JS. Proteinase systems and thoracic aortic aneurysm progression. *J Surg Res*. 2007;139:292–307. DOI: 10.1016/j.jss.2006.09.020.
31. Karimi A, Milewicz DM. Structure of the elastin-contractile units in the thoracic aorta and how genes that cause thoracic aortic aneurysms and dissections disrupt this structure. *Can J Cardiol*. 2016;32:26–34. DOI: 10.1016/j.cjca.2015.11.004.
32. Konrad L, Scheiber JA, Schwarz L, Schrader AJ, Hofmann R. TGF-beta1 and TGF-beta2 strongly enhance the secretion of plasminogen activator inhibitor-1 and matrix metalloproteinase-9 of the human prostate cancer cell line PC-3. *Regul Pept*. 2009;155:28–32.
33. Li Z, Zhou C, Tan L, Chen P, Cao Y, Li C, Li X, Yan J, Zeng H, Wang D-W, et al. Variants of genes encoding collagens and matrix metalloproteinase system increased the risk of aortic dissection. *Sci China Life Sci*. 2017;60:57–65. DOI: 10.1007/s11427-016-0333-3.
34. Nicholls AC, Oliver JE, McCarron S, Harrison JB, Greenspan DS, Pope FM. An exon skipping mutation of a type V collagen gene (COL5A1) in Ehlers-Danlos syndrome. *J Med Genet*. 1996;33:940–946. DOI: 10.1136/jmg.33.11.940.
35. Symoens S, Malfait F, Vlummens P, Hermanns-Le T, Syx D, De Paepe A. A novel splice variant in the N-propeptide of COL5A1 causes an EDS phenotype with severe kyphoscoliosis and eye involvement. *PLoS One*. 2011;6:e20121. DOI: 10.1371/journal.pone.0020121.
36. Malfait F, De Paepe A. Molecular genetics in classic ehlers-danlos syndrome. *Am J Med Genet C Semin Med Genet*. 2005;139C:17–23. DOI: 10.1002/ajmg.c.30070.
37. Chamberlain J, Gunn J, Francis SE, Holt CM, Arnold ND, Cumberland DC, Ferguson MW, Crossman DC. TGFbeta is active, and correlates with activators of TGFbeta, following porcine coronary angioplasty. *Cardiovasc Res*. 2001;50:125–136.
38. Nikol S, Isner JM, Pickering JG, Kearney M, Leclerc G, Weir L. Expression of transforming growth factor-beta 1 is increased in human vascular restenosis lesions. *J Clin Invest*. 1992;90:1582–1592. DOI: 10.1172/JCI116027.
39. Feng XH, Lin X, Derynck R. Smad2, Smad3 and Smad4 cooperate with Sp1 to induce p15(Ink4B) transcription in response to TGF-beta. *EMBO J*. 2000;19:5178–5193.
40. Ishii T, Asuwa N. Collagen and elastin degradation by matrix metalloproteinases and tissue inhibitors of matrix metalloproteinase in aortic dissection. *Hum Pathol*. 2000;31:640–646. DOI: 10.1053/hupa.2000.7642.
41. Kurihara T, Shimizu-Hirota R, Shimoda M, Adachi T, Shimizu H, Weiss SJ, Itoh H, Hori S, Aikawa N, Okada Y. Neutrophil-derived matrix metalloproteinase 9 triggers acute aortic dissection. *Circulation*. 2012;126:3070–3080. DOI: 10.1161/CIRCULATIONAHA.112.097097.
42. Chalouhi N, Hoh BL, Hasan D. Review of cerebral aneurysm formation, growth, and rupture. *Stroke*. 2013;44:3613–3622. DOI: 10.1161/STROKEAHA.113.002390.
43. Yamashiro Y, Yanagisawa H. Crossing bridges between extra- and intra-cellular events in thoracic aortic aneurysms. *J Atheroscler Thromb*. 2018;25:99–110. DOI: 10.5551/jat.RV17015.
44. Habashi JP, Judge DP, Holm TM, Cohn RD, Loeys BL, Cooper TK, Myers L, Klein EC, Liu G, Calvi C, et al. Losartan, an AT1 antagonist, prevents aortic aneurysm in a mouse model of Marfan syndrome. *Science*. 2006;312:117–121. DOI: 10.1126/science.1124287.
45. Habashi JP, Doyle JJ, Holm TM, Aziz H, Schoenhoff F, Bedja D, Chen Y, Modiri AN, Judge DP, Dietz HC. Angiotensin II type 2 receptor signaling attenuates aortic aneurysm in mice through ERK antagonism. *Science*. 2011;332:361–365. DOI: 10.1126/science.1192152.

SUPPLEMENTAL MATERIAL

Table S1. Selected 152 aortic dissection related genes for targeted sequencing.

No.	Gene	Official Full Name	Chr.	CDS, n	Amplicons, n	Target, bp	Coverage, %
1	*ABCC6*	ATP binding cassette subfamily C member 6	16	32	37	4903	100
2	*ACAT2*	acetyl-CoA acetyltransferase 2	6	9	10	1284	100
3	*ACTA2*	actin alpha 2, smooth muscle	10	8	10	1134	100
4	*ACVRL1*	activin A receptor like type 1	12	9	12	1602	100
5	*AKT1*	AKT serine/threonine kinase 1	14	13	18	1573	98.9
6	*AKT2*	AKT serine/threonine kinase 2	19	14	15	1576	100
7	*APOE*	apolipoprotein E	19	3	6	984	100
8	*APP*	amyloid beta precursor protein	21	20	19	2545	100
9	*ATM*	ATM serine/threonine kinase	11	62	70	9791	100
10	*BRCC3*	BRCA1/BRCA2-containing complex subunit	X	12	11	1064	100

11	*CBS*	cystathionine-beta-synthase	21	15	18	1806	100
12	*CCM2*	CCM2 scaffold protein	7	11	14	1538	100
13	*CDKN2A*	cyclin dependent kinase inhibitor 2A	9	7	9	1345	100
14	*CDKN2B*	cyclin dependent kinase inhibitor 2B	9	3	4	687	100
15	*COL10A1*	collagen type X alpha 1 chain	6	2	10	2063	100
16	*COL11A1*	collagen type XI alpha 1 chain	1	68	69	6254	99.7
17	*COL11A2*	collagen type XI alpha 2 chain	6	67	62	5946	100
18	*COL12A1*	collagen type XII alpha 1 chain	6	65	75	9842	100
19	*COL13A1*	collagen type XIII alpha 1 chain	10	40	40	2554	100
20	*COL14A1*	collagen type XIV alpha 1 chain	8	47	49	5861	100
21	*COL15A1*	collagen type XV alpha 1 chain	9	42	43	4587	100
22	*COL16A1*	collagen type XVI alpha 1 chain	1	70	67	5515	99.8
23	*COL17A1*	collagen type XVII alpha 1 chain	10	55	56	5044	100

24	*COL18A1*	collagen type XVIII alpha 1 chain	21	44	52	5096	96.3
25	*COL19A1*	collagen type XIX alpha 1 chain	6	50	51	3929	100
26	*COL1A1*	collagen type I alpha 1 chain	17	51	56	4956	99.01
27	*COL1A2*	collagen type I alpha 2 chain	7	52	48	4621	94.3
28	*COL20A1*	collagen type XX alpha 1 chain	20	34	42	4195	97.8
29	*COL21A1*	collagen type XXI alpha 1 chain	6	29	32	3164	100
30	*COL22A1*	collagen type XXII alpha 1 chain	8	64	67	5521	100
31	*COL23A1*	collagen type XXIII alpha 1 chain	5	29	27	1913	84.1
32	*COL24A1*	collagen type XXIV alpha 1 chain	1	60	68	5745	97.9
33	*COL25A1*	collagen type XXV alpha 1 chain	4	40	42	2616	100
34	*COL26A1*	collagen type XXVI alpha 1 chain	7	14	16	1455	95.1
35	*COL27A1*	collagen type XXVII alpha 1 chain	9	61	70	6193	100
36	*COL28A1*	collagen type XXVIII alpha 1 chain	7	34	37	3718	100

37	*COL2A1*	collagen type II alpha 1 chain	12	54	56	5004	97.8
38	*COL3A1*	collagen type III alpha 1 chain	2	51	71	4401	97.8
39	*COL4A1*	collagen type IV alpha 1 chain	13	52	51	5530	100
40	*COL4A2*	collagen type IV alpha 2 chain	13	47	50	5609	99.6
41	*COL4A3*	collagen type IV alpha 3 chain	2	52	53	5533	100
42	*COL4A3 BP*	collagen type IV alpha 3 binding protein	5	19	19	2439	100
43	*COL4A4*	collagen type IV alpha 4 chain	2	47	49	5543	99.9
44	*COL4A5*	collagen type IV alpha 5 chain	X	53	53	5573	98.2
45	*COL4A6*	collagen type IV alpha 6 chain	X	47	48	5608	100
46	*COL5A1*	collagen type V alpha 1 chain	9	66	76	6243	98.35
47	*COL5A2*	collagen type V alpha 2 chain	2	54	68	5094	98.35
48	*COL5A3*	collagen type V alpha 3 chain	19	67	62	5908	95.9

49	*COL6A1*	collagen type VI alpha 1 chain	21	35	38	3437	95.6
50	*COL6A2*	collagen type VI alpha 2 chain	21	29	37	3672	96.9
51	*COL6A3*	collagen type VI alpha 3 chain	2	44	63	10011	100
52	*COL6A5*	collagen type VI alpha 5 chain	3	41	54	8245	98.5
53	*COL6A6*	collagen type VI alpha 6 chain	3	36	47	7152	100
54	*COL7A1*	collagen type VII alpha 1 chain	3	118	96	10015	95.6
55	*COL8A1*	collagen type VIII alpha 1 chain	3	2	11	2255	99.2
56	*COL8A2*	collagen type VIII alpha 2 chain	1	2	10	2132	97.6
57	*COL9A1*	collagen type IX alpha 1 chain	6	39	38	3228	99.6
58	*COL9A2*	collagen type IX alpha 2 chain	1	32	29	2390	99.8
59	*COL9A3*	collagen type IX alpha 3 chain	20	32	30	2375	93.6
60	*CST3*	cystatin C	20	3	4	471	100
61	*CTGF*	connective tissue growth factor	6	5	9	1105	93.57

62	*ELN*	elastin	7	38	32	2734	100
63	*ENG*	endoglin	9	17	18	2153	100
64	*FBN1*	fibrillin 1	15	65	98	8616	99.7
65	*FBN2*	fibrillin 2	5	65	71	9389	100
66	*FBN3*	fibrillin 3	19	63	75	9060	97.5
67	*FLNA*	filamin A	X	47	70	8461	100
68	*GLA*	galactosidase alpha	X	7	7	1360	100
69	*GLMN*	glomulin, FKBP associated protein	1	18	20	1965	100
70	*HBB*	hemoglobin subunit beta	11	3	3	474	100
71	*HTRA1*	HtrA serine peptidase 1	10	9	11	1533	95
72	*ITGB1*	integrin subunit beta 1	10	16	19	2632	100
73	*ITGB4*	integrin subunit beta 4	17	40	52	6028	93.5
74	*ITGB5*	integrin subunit beta 5	3	15	18	2550	96.9

75	*ITGB6*	integrin subunit beta 6	2	18	16	2517	100
76	*ITGB7*	integrin subunit beta 7	12	14	14	2537	100
77	*ITGB8*	integrin subunit beta 8	7	14	17	2450	100
78	*ITM2B*	integral membrane protein 2B	13	6	7	861	100
79	*KRIT1*	KRIT1 ankyrin repeat containing	7	16	23	2371	100
80	*MMP1*	matrix metallopeptidase 1	11	11	14	1683	100
81	*MMP10*	matrix metallopeptidase 10	11	10	11	1531	100
82	*MMP11*	matrix metallopeptidase 11	22	8	12	1547	100
83	*MMP12*	matrix metallopeptidase 12	11	10	16	1522	99.74
84	*MMP13*	matrix metallopeptidase 13	11	10	12	1516	100
85	*MMP14*	matrix metallopeptidase 14	14	10	13	1849	100
86	*MMP15*	matrix metallopeptidase 15	16	10	17	2110	99.7
87	*MMP16*	matrix metallopeptidase 16	8	10	13	1924	100

88	*MMP17*	matrix metallopeptidase 17	12	10	16	1912	89.3
89	*MMP19*	matrix metallopeptidase 19	12	11	10	1723	100
90	*MMP2*	matrix metallopeptidase 2	16	14	18	2140	98.79
91	*MMP20*	matrix metallopeptidase 20	11	10	10	1552	100
92	*MMP21*	matrix metallopeptidase 21	10	7	11	1780	98.8
93	*MMP22*	matrix metallopeptidase 22	1	8	8	1253	85.3
94	*MMP24*	matrix metallopeptidase 24	20	9	12	2028	87.4
95	*MMP25*	matrix metallopeptidase 25	16	10	12	1789	85.4
96	*MMP26*	matrix metallopeptidase 26	11	6	6	846	100
97	*MMP27*	matrix metallopeptidase 27	11	10	12	1642	100
98	*MMP28*	matrix metallopeptidase 28	17	9	11	1656	100
99	*MMP3*	matrix metallopeptidase 3	11	10	15	1544	100
100	*MMP7*	matrix metallopeptidase 7	11	6	6	864	100

101	*MMP8*	matrix metallopeptidase 8	11	10	14	1514	97.89
102	*MMP9*	matrix metallopeptidase 9	20	13	18	2267	99.34
103	*MSTN*	myostatin	2	3	10	1161	99.4
104	*MYH1*	myosin heavy chain 1	17	38	40	6200	97.8
105	*MYH10*	myosin heavy chain 10	17	43	48	6444	100
106	*MYH11*	myosin heavy chain 11	16	42	62	5971	99.4
107	*MYH13*	myosin heavy chain 13	17	39	42	6207	99.4
108	*MYH14*	myosin heavy chain 14	19	42	50	6531	100
109	*MYH15*	myosin heavy chain 15	3	42	44	6261	100
110	*MYH2*	myosin heavy chain 2	17	38	39	6206	99.4
111	*MYH3*	myosin heavy chain 3	17	39	43	6213	99.3
112	*MYH4*	myosin heavy chain 4	17	38	42	6200	100
113	*MYH8*	myosin heavy chain 8	17	38	41	6194	99.4

114	*MYLK*	myosin light chain kinase	3	33	50	5962	100
115	*MYLK2*	myosin light chain kinase 2	20	12	17	1911	100
116	*MYLK3*	myosin light chain kinase 3	16	13	17	2590	100
117	*NF1*	neurofibromin 1	17	59	70	9161	99
118	*NOTCH1*	notch receptor 1	9	34	67	7668	97.9
119	*NOTCH2*	notch receptor 2	1	35	42	7809	100
120	*NOTCH3*	notch receptor 3	19	33	42	7296	87.4
121	*NOTCH4*	notch receptor 4	6	30	40	6312	99.7
122	*PDCD10*	programmed cell death 10	3	7	7	709	100
123	*PLOD1*	programmed cell death 1	1	19	21	2184	99.9
124	*PLOD3*	programmed cell death 3	7	19	23	2407	96.9
125	*PRNP*	prion protein	20	2	3	772	100
126	*PTEN*	phosphatase and tensin homolog	10	9	11	1302	100

127	*RASA1*	RAS p21 protein activator 1	5	26	34	3412	100
128	*RNF213*	ring finger protein 213	17	68	96	16462	100
129	*S100A12*	S100 calcium binding protein A12	1	2	2	301	100
130	*SLC2A10*	S100 calcium binding protein A10	20	5	16	1626	100
131	*SMAD1*	SMAD family member 1	4	6	8	1458	100
132	*SMAD2*	SMAD family member 2	18	10	15	1514	100
133	*SMAD3*	SMAD family member 3	15	12	15	1459	100
134	*SMAD4*	SMAD family member 4	18	11	19	1780	98.76
135	*SMAD5*	SMAD family member 5	5	6	9	1457	100
136	*SMAD6*	SMAD family member 6	15	5	11	1575	98.9
137	*SMAD7*	SMAD family member 7	18	7	9	1630	100
138	*SMAD9*	SMAD family member 9	13	6	7	1464	100
139	*TGFA*	transforming growth factor alpha	2	7	6	543	100

140	*TGFB1*	transforming growth factor beta 1	19	7	11	1250	100
141	*TGFB2*	transforming growth factor beta 2	1	8	13	1329	98.6
142	*TGFB3*	transforming growth factor beta 3	14	7	9	1309	100
143	*TGFBR1*	transforming growth factor beta receptor 1	9	9	17	1512	92.3
144	*TGFBR2*	transforming growth factor beta receptor 2	3	8	16	1779	96.5
145	*TGFBR3*	transforming growth factor beta receptor 3	1	17	19	2716	100
146	*TIE2*	TEK receptor tyrosine kinase	9	23	25	3605	100
147	*TIMP1*	TIMP metallopeptidase inhibitor 1	X	5	5	674	100
148	*TIMP2*	TIMP metallopeptidase inhibitor 2	17	5	6	713	100
149	*TIMP3*	TIMP metallopeptidase inhibitor 3	22	5	5	686	100
150	*TIMP4*	TIMP metallopeptidase inhibitor 4	3	5	5	725	100
151	*TREX1*	three prime repair exonuclease 1	3	3	5	1120	100
152	*TTR*	transthyretin	18	4	4	484	100

No., number; Chr., chromosome; CDS, coding sequence

Table S2. Primers used in this study.

Name	Forward	Reverse
Rat-COL5A1-validation	5'-TTTTCTTTGATTAGCTTACTGACGAGG-3'	5'-GTGACAACTGTGGGGTAGATGTG-3'
Rat-Cre-validation	5'-TACTGACGGTGGGAGAATG-3'	5'-CTGTTTCACTATCCAGGTTACG-3'

Table S3. The baseline information of rats.

	WT	*Col5a1*$^{+/-}$	*Col5a1*$^{-/-}$
N	14	26	0
BW (g)	116.3±7.9	97.8±16.8*	NA
SBP (mmHg)	112.4±6.8	113.0±4.0	NA
DBP (mmHg)	86.0±5.2	84.6±3.1	NA

WT, wild type; N, born numbers; SBP, systolic blood pressure; DBP, diastolic blood pressure; NA, not available; *indicated $p < 0.05$.

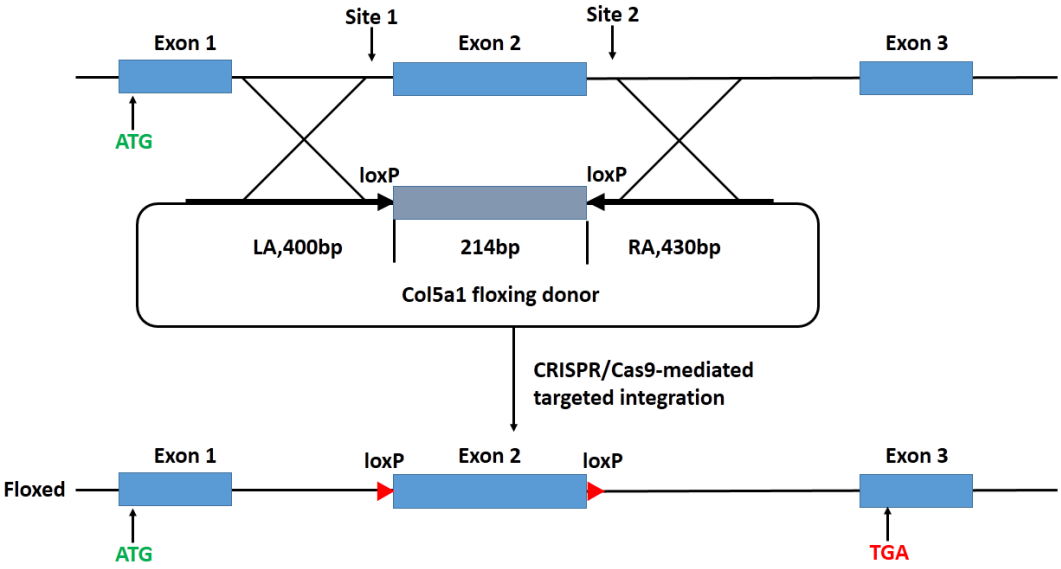

Figure S1. Generation of *Col5a1*$^{fl/fl}$ rats using CRISPR/Cas9 system. The loxP sequence was inserted upstream and downstream of exon 2, and exon 2 were deleted after mating of Col5a1$^{fl/fl}$ and transgenic cre rats, which generated a new termination codon TGA in exon 3.

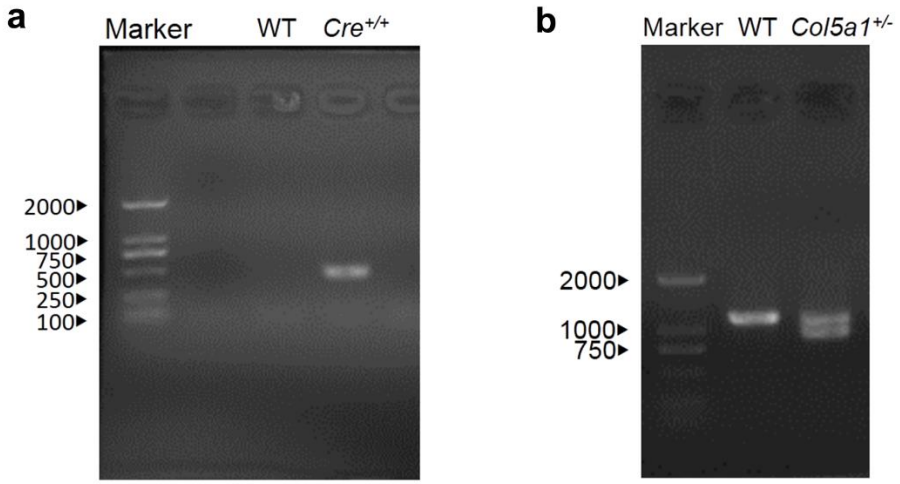

Figure S2. (a) The validation of cre transgenic rats using DNA agarose gel electrophoresis. **(b)** The validation of *Col5a1*$^{+/-}$ rats using DNA agarose gel electrophoresis. WT, wild type.

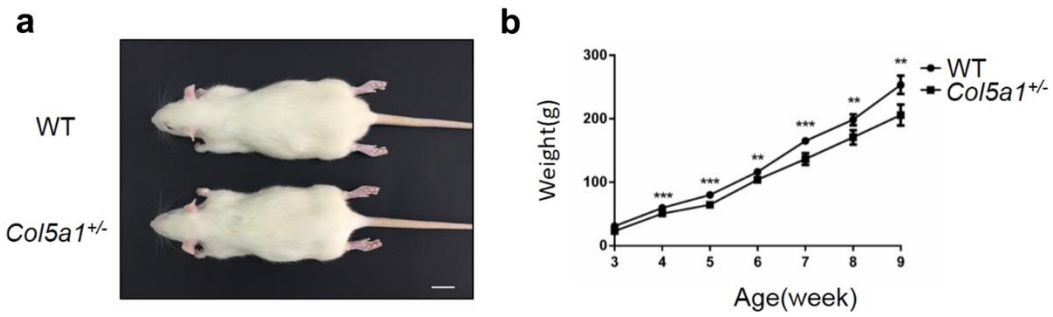

Figure S3. (a) Status of development of 9-week-old WT and *Col5a1*$^{+/-}$ rats. Scale bar: 1cm. **(b)** Body weight of WT and *Col5a1*$^{+/-}$ rats at 3-9 week of age. **indicated $p<0.01$; ***indicated $p<0.001$. WT, wild type.

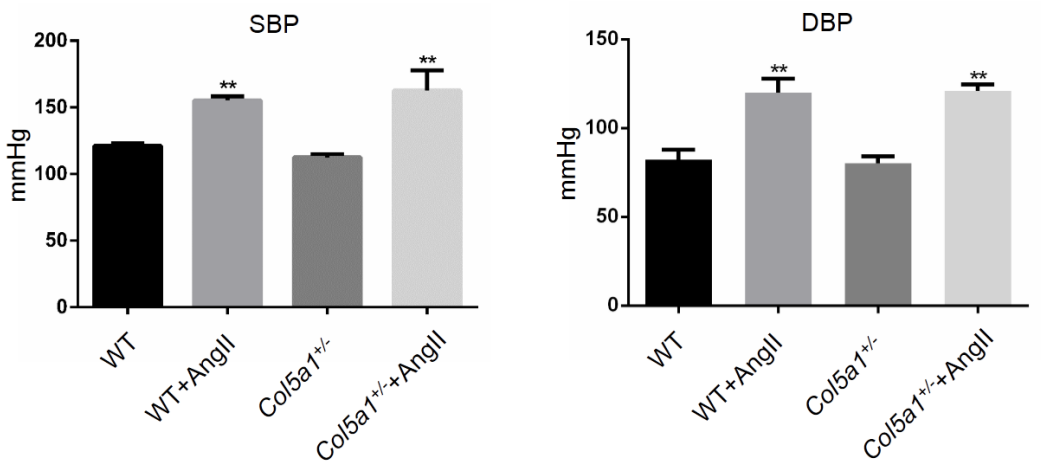

Figure S4. After treated with AngII, SBP and DBP increased significantly in both WT and *Col5a1*$^{+/-}$ rats, the blood pressure in the corresponding groups showed no significant difference. **indicated $p<0.01$. WT, wild type; AngII angiotensin II; BAPN, β-aminopropionitrile monofumarate ; SBP, systolic blood pressure; DBP, diastolic blood pressure.

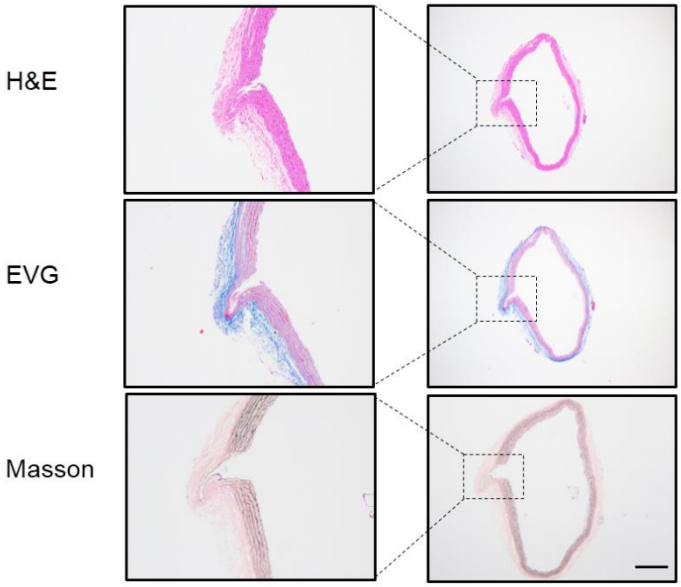

Figure S5. The aortic aneurysm was observed in *Col5a1*$^{+/-}$ rat after treated with BAPN alone for 4 weeks.